Journal of Materials Chemistry C

RSC Publishing

PAPER

View Article Online
View Journal | View Issue

Cite this: J. Mater. Chem. C, 2013, 1, 6395

Towards inkjet-printed low cost passive UHF RFID skin mounted tattoo paper tags based on silver nanoparticle inks†

Veronica Sanchez-Romaguera,*[a] Mohamed A. Ziai,[b] Dumtoochukwu Oyeka,[b] Silvia Barbosa,[c] Joseph S. R. Wheeler,[a] John C. Batchelor,[b] Edward. A. Parker[b] and Stephen G. Yeates*[a]

Received 8th July 2013
Accepted 19th August 2013

DOI: 10.1039/c3tc31302f

www.rsc.org/MaterialsC

The present work describes the inkjet printing and low temperature sintering of silver nanoparticle inks onto transfer tattoo paper. Our approach results in silver features of excellent resolution and conductivity and, subsequently the first passive UHF RFID transfer tattoo tags functional mounted on human skin of improved performance when compared to screen printed passive UHF RFID transfer tattoo paper tags. Moreover, inkjet printed passive UHF RFID transfer tattoo tags show similar performance to copper etched passive UHF RFID tags on plastic substrates. This study compares the image quality (resolution) and electrical performance of two commercial silver nanoparticle inks inkjet printed on transfer tattoo paper. The optimal printing and sintering parameters to obtain high resolution features of resistivities 20 to 57 times the resistivity of bulk silver (1.59×10^{-6} ohm cm) are described. We demonstrate how, by selectively depositing ink in specific areas of the antenna, read distance of passive UHF RFID tags can be increased from 54 to 68 cm whilst decreasing the amount of ink used by 33%. Furthermore, this approach results in inkjet printed passive UHF RFID tattoo tags with larger read distance than silver screen printed passive UHF RFID tattoo tags, 45 cm, and similar to copper etched passive UHF RFID plastic tags, 75 cm. Moreover, inkjet printed passive UHF RFID tattoo tags in this work are considerably thinner (1–5 μm) than screen and etched passive UHF RFID tags (tens of micrometers) hence, making the former more appealing to the end user. In addition to this, inkjet printing is compatible with large area manufacturing techniques and has the potential to evolve as one of the most promising RFID mass-production techniques. Therefore, this work represents a step towards the commercialization of *on-body* transfer tattoo paper passive UHF RFID tags.

1 Introduction

The use of passive RFID tags in asset management is well documented and its use in monitoring, identifying and tracking people particularly in work environments such as power plants, airports, hospitals, military bases, refineries and access restricted areas is emerging.[1–5] Current human tagging and monitoring technology, external to the body, typically requires bulky wrist bands or ID badges which can be easily transferred among users compromising security related application. Some monitoring applications rely on electrodes mounted on the skin *via* adhesive tapes, straps, or penetrating needles, often aided by a conductive gel, with terminal connections to separate boxes hosting circuit boards, power supplies and communication components, all of which are poorly suited for practical applications outside of research labs or clinical setting.[6,7] In response to the growing interest in non-intrusive human tagging and monitoring, there has been intensive research in the areas of electronic skin (electronic like skin) and on-skin electronics (electronics mounted on skin).

Recent work in the area of *electronic skin* includes work from Dae-Hyeong Kim *et al.*[8] demonstrating the possibility to attach high-performance electronic functionalities to the surface of the skin. Here a collection of sensors, circuit elements and radio-frequency (RF) communication components was patterned by a combination of spin-coating, photolithography, dry etching and transfer printing onto the surface of a carefully engineered thin, lightweight, stretchable "skin-like" conformal silicone and polyvinyl alcohol (PVA) substrates. Transfer of the electronic components onto the surface of the skin was then achieved by soft contact in a similar manner to a temporary transfer tattoo.

[a]Organic Materials Innovation Centre (OMIC), School of Chemistry, The University of Manchester, M15 5AX, Manchester, UK. E-mail: Veronica.Sanchez@manchester.ac.uk; Fax: +44 (0)1612754273; Tel: +44 (0)1612753896

[b]School of Engineering and Digital Arts, University of Kent, CT2 7NT, Kent, UK. E-mail: J.C.Batchelor@kent.ac.uk; Fax: +44 (0)1227 456084; Tel: +44 (0)1227 827004

[c]Condensed Matter Physics Department, Faculty of Physics, Universidade de Santiago de Compostela, 15782, Santiago de Compostela, Spain. E-mail: silvia.barbosa@usc.es; Fax: +34 981 520676; Tel: +34 981 563100

† Electronic supplementary information (ESI) available. See DOI: 10.1039/c3tc31302f

In terms of *on-skin* electronics, RFID tags operating at ultra-high frequencies (UHF), 860–960 MHz, are of particular interest because of their superior read distance (up to 10 metres) and potential to be very cheap compare to other passive RFID tags such as those operating at high frequency (HF), 13.56 MHz, or low frequency (LF) 125 kHz.[1] However, passive UHF RFID tags mounted directly onto skin are particularly challenging due to the intrinsic electrical characteristics of the human body which can interfere with RF components.[9] Recently J. C. Batchelor *et al.* successfully engineered a substrate insensitive *thin* antenna and demonstrated the first temporary on-skin passive UHF RFID tag fabricated on transfer tattoo paper by stencil printing means.[10,11] These *on-skin* wireless UHF RFID tags constitute a considerable step forwards towards a deployable UHF RFID system for human tagging and monitoring. However, in order to make this technology commercially viable it is important to keep the operational cost per antenna as low as possible. Whilst wet etch processing is able to reliably produce copper tracks of high conductive and edge definition thus yielding UHF RFID tags of excellent performance (read distance), the corrosive nature of solvents used in the etching process makes this technology not suited to substrates such as paper. A prototype *on-skin* UHF RFID transfer tattoo tag using a stencil technique was first described by M. A. Ziai *et al.*[12] and whilst suited for transfer tattoo paper, resulted in tags with visibly poor edge definition and shorter read distances than etched tags since poor tag definition and any deviations from antenna nominal dimensions have an impact effect on tag performance.[10] Thus, an alternative technique is needed if low-cost UHF RFID tattoo tags are to be realized.

Inkjet printing offers a number of potential benefits: (1) no need for masks and therefore, pattern designs can be readily altered making it a powerful rapid prototyping technology, (2) compatible with porous paper-like substrates and (3) enables multilayer deposition of the same or different fluids with unique spatial resolution. However a number of challenges need to be addressed if inkjet printing for UHF RFID applications is to become a reality. Chief amongst these is achieving high conductivity on a porous, rough and temperature sensitive tattoo substrate with high image quality.

Whilst developments in the field of *on-skin* mounted electronics and inkjet printing of UHF RFID tags on paper have recently emerged,[13–15] to our knowledge no research has been reported combining both fields.

Here we introduce an investigation to determine the feasibility of obtaining low-cost thin passive UHF RFID transfer tattoo tags by combining inkjet printable low temperature thermal sintering silver precursor inks on tattoo paper. In this process the UHF RFID tag is sandwiched between two layers of polymeric nature originating from the tattoo paper. Therefore, there is no direct contact between the silver tag and the body upon transfer onto the body.

2 Experimental section

Materials

Two commercial silver nanoparticle dispersions were used in this work. Ink A, was a dispersion in water from Novacentrix (Metalon JS-B25HV) containing 25 wt% of silver nanoparticles, with a particle size diameter of 60 nm determined by Dynamic Light Scattering (DLS). Ink B, was a dispersion in ethanol–ethylene glycol mixture from Sigma-Aldrich (SunTronic U5603 from Sun Chemicals) containing 20 wt% of silver nanoparticles, with a particle size diameter of 30–50 nm.[16] Inkjet tattoo paper was supplied by http://www.craftycomputerpaper.co.uk and purged with a flow of air to remove dust particles. Conventional microscope glass slides (2.54 × 7.62 cm; Sailing Boat, Cat. no. 7101, China) were used and ultra-sonicated for 10 minutes in an acetone bath, rinsed with deionized water and placed in a convection oven at 60 °C for 10 minutes prior to use.

The RFID integrated circuit chip used on the all the tag designs was an NXP RFID ASIC (Application Specific Integrated Circuit) mounted on copper straps for contact with the RFID metal antenna. The NXP chip (NXP Semiconductors, Stockport, UK) had a high frequency input impedance consisting of a resistive part, 15 ohm, and a capacitive component equal to 128 ohm at the RFID frequency. The RFID integrated circuit was connected to the metal antenna by direct ohmic contact and mechanically attached to the antenna by proprietary adhesive tape. The ohmic contact was achieved by applying point pressure to the copper straps and the underlying printed conductor.

Instruments

Inkjet printing was performed using a piezoelectric Dimatix DMP-2800 system (Dimatix-Fujifilm Inc., USA), equipped with a 10 pL cartridge (DMC-11610). The nozzle plate consists of a single raw of 16 nozzles of 23 μm diameter spaced 254 μm. The print head contains a row of 16 nozzles. Printhead height was set to 1 mm and the printer platen temperature 50 °C unless otherwise stated. Ink A jetted reliably at 30 °C using a 22 V waveform whereas Ink B jetted reliably at 38 °C using a 20 V waveform. Thermal sintering was carried out on a hot plate. Sintering temperature was 135 °C unless otherwise stated. Sintering times between 15 and 120 minutes were used to study resistance as function of sintering time. Thermogravimetric analysis (TGA) was performed under ambient atmosphere in the range from room temperature to 600 °C with heating rate of 10 °C min^{-1} using a TGAQ5000 system from TA Instruments. Differential scanning calorimetry (DSC) measurements were recorded using a Perkin Elmer Jade DSC instrument under nitrogen atmosphere, 5–10 mg of the sample was sealed in an aluminum pan with a crimping tool. The sample was heated from 25 °C to 200 °C at a heating rate of 10 °C min^{-1}, held for 5 minutes at 200 °C and then cooled to 25 °C at a rate of 10 °C min^{-1}. This cycle was repeated three times. The electrical resistance of sintered silver features was measure by the 4-point probe technique. Grazing angle FT-IR experiments were performed on a Bruker Vertex-70 spectrometer equipped with a Harrick Seagull accessory and Germanium hemisphere ATR crystal and nitrogen purge. The sample was mounted with a torque of 7.4 in. lb and incident angle of 65°. Both background and measurements were averaged over 64 scans with a resolution of 4 cm^{-1}, recorded by a DLaTGS detector. A Jandel multi-position wafer probe system (Jandel Engineering Ltd., Leighton

Buzzard, UK) mounted with a cylindrical probe head (solid tungsten carbide needles of 0.40 mm diameter spaced 1.0 mm) was employed. Surface topography, thickness, and cross-sectional areas of the printed silver tracks were measured with an optical profilometer (Dektak Veecko32). Scanning electron microscopy (SEM) images were taken using a EVO®LS 15 system (Carl Zeiss Microscopy, Germany) operating at an accelerating voltage of 20 kV. Tag read distance was measured using a Voyantic Tagformance lite RFID measurement system (Voyantic Ltd., Finland). After calibrating the system at 35 cm the RFID tag was transferred to the volunteers arm and the read range was extrapolated by measurement at the global RFID UHF frequency bands within permitted transmission power levels.

3 Results and discussions

The thermal stability of the commercially available tattoo paper used in this work was evaluated. A schematic of the various layers of tattoo paper and the steps to produce and transfer an UHF RFID tattoo tag on human body are described in Fig. 1. As shown in Fig. 1b, the thermogravimetric analysis (TGA) of the ink receiving layer of tattoo paper shows an initial mass loss at approximately 100 °C attributed to the loss of adsorbed moisture, with further mass losses observed between 225 and 685 °C. The various mass loss steps between 225 and 685 °C are attributed to the decomposition of the various components within the ink receiving layer. This suggests that after an initial dehydration step of 8 wt%, thermal decomposition does not begin until 225 °C. Transfer tattoo paper shape and color changes were visually assessed as a function of temperature. At 150 °C within less than 15 minutes tattoo paper changed from white to a yellow-brownish colour, however at 140 °C to the naked eye there was no change in color or in shape during an 8 hours period. Based on these results, in order to ensure transfer tattoo paper did not change color during the heating process, a slightly lower temperature: 135 °C was adopted as the sintering temperature in this work unless otherwise stated.

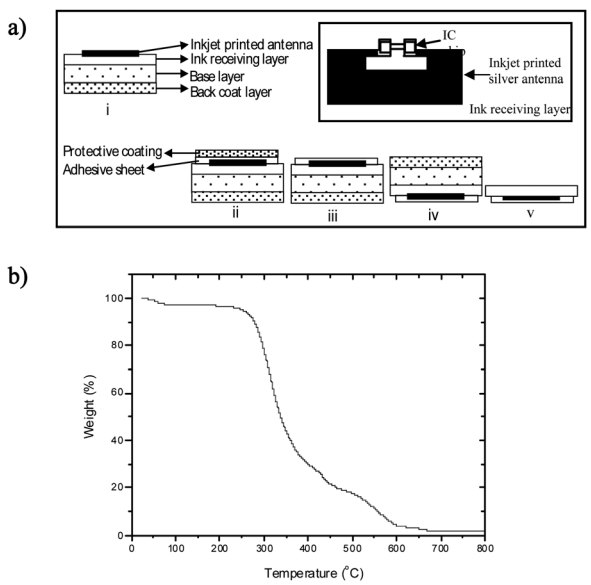

Fig. 1 (a) Schematic of the formation and transfer of an inkjet printed RFID tag onto the body. (i) The UHF RFID antenna pattern is inkjet printed onto the ink-receiving layer. Upon sintering, the IC chip is attached to the ports of the antenna in order to form the UHF RFID tag. Then, (ii) the adhesive sheet with protective coating is applied to the printed UHF RFID tag, (iii) the protective coating is removed, (iv) the tattoo is flipped and applied to the skin and moistened with water, and (v) the base and back coat paper layers are removed. (b) Thermogravimetric analysis of transfer paper.

Two commercially available metal precursor inks, Ink A (Novacentrix, Metalon JS-B25HV) and Ink B (Sigma-Aldrich, SunTronic U5603 from Sun Chemicals), were selected on their potential to thermally sinter at temperatures <150 °C (see TGA of inks in the ESI†, Fig. 1). We must point out that, as stated by the ink suppliers, the resultant conductivity depends both upon sintering time, temperature and also substrate and hence may not demonstrate optimal performance on the substrate used in this study.[17,18] Preliminary inkjet printing experiments were carried out to assess the image quality (print edge definition) of the selected inks on tattoo paper and line conductivity. Simple structures were inkjet printed onto the substrate at 25 °C and immediately heated at 135 °C for 30 minutes. Printing at the same dot spacing Ink A yielded narrower features than Ink B, the difference being explained in terms of substrate wetting behavior as contact angle on tattoo paper for Ink A and Ink B are respectively 35 and 12 degrees. Dot spacing resulting in pin-hole free continuous features was optimized for both inks. Upon sintering, Ink A showed exceptional line definition over a range of dot spacing's tested (10–30 μm). Upon sintering Ink A changed from brown, "as-printed", to bluish but the features remained non-conductive. The bluish color of silver nanoparticle features has been attributed to an absence of sintered nanoparticles.[19] In an attempt to obtain silver mirror-like conductive lines the as-printed features were sintered at 135 °C for a period of up to 2 hours. However, as shown in Fig. 2a, features remained bluish and non-conductive. Due to sintering temperature limitations imposed by the substrate sintering at higher temperatures was not investigated and despite the excellent image quality achieved, no further work was carried out with Ink A. Regardless of dot spacing, Ink B yielded features of poor edge definition as shown in Fig. 2b. During the heating process the printed features underwent various color changes from brown, as-printed, to shinny silver mirror-like features within seconds upon contact with the hot plate with conductive features being obtained upon sintering at 135 °C for 30 minutes. Consequently all further work focused upon Ink B.

In an attempt to improve image quality of Ink B features on tattoo paper inkjet printing was carried out on pre-heated tattoo paper, with the printer platen set at 50 °C. Tattoo paper was placed on the platen for 30 minutes prior to printing. Inkjet printing onto warm substrate resulted in a substantial improvement in image quality, as shown in Fig. 2c. It has been reported before that ink droplet spreading can be limited by pre-heating the substrate to temperatures between 40 and 70 °C range caused by an increase in viscosity due to rapid evaporation of volatiles within the ink.[20] According to the ink specifications, Ink B is an ethanol–ethylene glycol based ink, with TGA showing a gradual initial mass loss of 9 wt% at approx. 50 °C

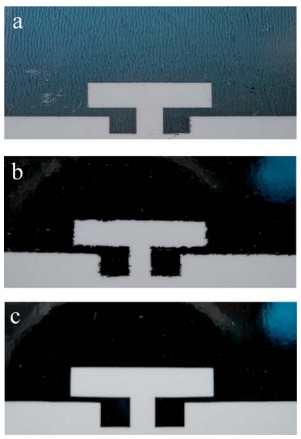

Fig. 2 Photographs of inkjet printed silver antennas (a) using Ink A onto 25 °C transfer tattoo paper and heated at 135 °C for 2 hours, (b) using Ink B onto 25 °C transfer tattoo paper and heated at 135 °C for 30 min and (c) using Ink B onto 50 °C transfer tattoo paper and heated at 135 °C for 30 min.

which is attributed to ethanol evaporation. The improvement of image quality upon printing on heated tattoo paper is attributed to the instant evaporation of ethanol present in the ink upon reaching the warm substrate. We must point out that during the printing process the distance between the printhead and the substrate was set at 1 mm, typically used in inkjet printing. Although printing onto a warm substrate did improve resolution on occasions nozzle clogging and conversion on the nozzle plate were observed due to solvent evaporation on the nozzle plate. This issue could potentially be avoided by increasing the distance between the printhead and the substrate.

Comparison of inkjet printed lines with stencil printing and wet etching methods previously employed to fabricate UHF RFID tags of identical design[10,11] was carried out. In order to quantify and compare the resolution of the various deposition techniques simple lines of 500 μm nominal line width (NLW) were inkjet printed onto 25 °C and 50 °C tattoo paper substrates and thermally sintered at 135 °C for 30 minutes. Optical profilometry was used to determine the real line width (RLW) of lines produced by all three techniques. RLW was compared to the NLW using the following equation: line width gain (LWG)% = ((RLW − NLW)/NLW) × 100. Etched line resulted in the smallest LWG%, *circa* 10% (550 ± 3 μm line width) compared to approx. 25% (625 ± 5 μm) for line inkjet printing onto tattoo paper at 25 °C and over 100% (over 1000 ± 78 μm) for stencil printing line on 25 °C tattoo paper. Although from an image quality point of view wet etching is a powerful patterning tool, the corrosive nature of the solvents employed during the etching process makes this technique not suitable for paper substrates. Stencil printing processes, on the other hand, although suited for paper substrates lacked of the resolution required for certain RFID applications. By inkjet printing on pre-heated tattoo paper at 50 °C, LWG% of inkjet printed lines decreased from approx. 25% (625 ± 5 μm) to approx. 12% (560 ± 5 μm) thus resulting in an image quality similar to that achieved by wet etching. Based on these results, unless otherwise stated, the printer platen was set at 50 °C for further inkjet printing experiments.

Upon optimizing the inkjet printing conditions to obtain good image quality of the silver nanoparticle ink on tattoo paper its electrical performance was investigated quantitatively, and for comparison, inkjet printing onto glass substrate was also carried out. In order to investigate the effect of print thickness single and double pass lines (0.8 cm × 0.5 mm) and squares (1 cm × 1 cm) were inkjet printed at dot spacing settings of 15 and 20 μm chosen because they yielded continuous silver features (pin-hole free) and good resolution. Despite the immediate ink color change from brown to mirror-like silver upon contact with the warm substrate none of the "as-printed" features was found to be conductive at this stage. Upon printing, "as-printed" features were subsequently sintered on a hot plate pre-heated at 135 °C for between 15 and 120 minutes. For double pass structures sintering was performed after deposition of the second layer. Optical profilometry was used to determine the cross-sectional profile (A) of resulting features. Electrical resistivity ρ was calculated using the equation $\rho = RA/l$, where R is the resistance, l the length and A the cross-sectional area of the print.

Fig. 3a shows the resistivity of inkjet printed structures expressed as multiples of the resistivity of bulk silver as a function of heating time upon thermal sintering on glass substrates. As can be seen, a gradual decrease in resistivity as sintering time increases occurs regardless of dot spacing and number of ink layers deposited. This plot is typically observed when sintering silver nanoparticles on non-porous substrate such as glass and foils. The gradual decrease in resistivity rather than being abrupt is attributed the low sintering temperature, 135 °C. At short sintering times ≤30 minutes resistivity values are ×17–40 times of bulk silver, which is 2.5–11.6% of bulk silver conductivity. It is noticeable that the ink sinters readily after 15 minutes although the conductivity may not be sufficient for certain applications. Regardless of the amount of material deposited, 120 minutes sintering yields the lowest resistivity values, approx. ×3 times of bulk silver (33% of the bulk silver conductivity).

Fig. 3b shows the resistivity, expressed as multiples of the resistivity of bulk silver, of features inkjet printed onto tattoo paper, as a function of heating time. Unlike on glass, on tattoo paper two resistivity regimes are observed. *Regime I* corresponds to sintering times up to 30 minutes and *Regime II* corresponds to sintering times above 30 minutes. In *Regime I* the electrical performance of silver features on tattoo paper follows a similar trend to that observed for features printed on glass and the resistivity of silver features decreases as the heating time increases. Resistivity values within this regime varied between ×20–57 times the resistivity of bulk silver depending upon the dot spacing and the number of layers deposited. In *Regime II*, except in the case of features comprising 2 layers of materials printed at 15 μm dot spacing which follow the same resistivity trend as those printed on glass, all the other features showed either a minimum decrease of resistivity (15 μm_×1 layer, 20 μm_×1 layer) or an increase (20 μm_×1 layer) in resistivity as the heating time increased beyond 30 minutes. After 45 minutes

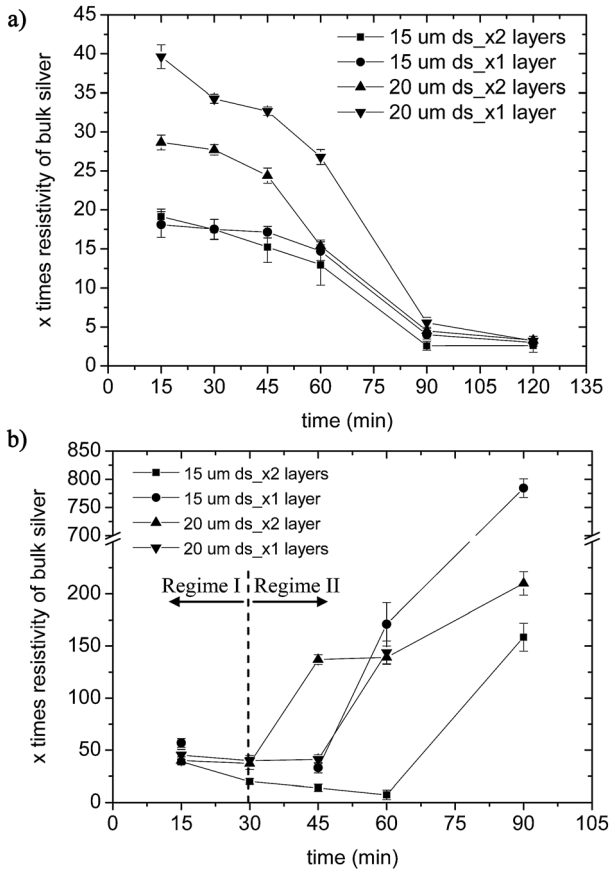

Fig. 3 Resistivity of silver features (expressed as multiples of the resistivity of bulk silver) as a function of heating time (a) inkjet printed on glass and (b) on transfer tattoo paper.

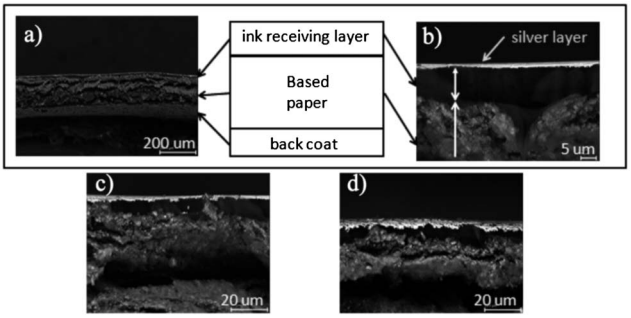

Fig. 4 SEM images of cross-sectional profile of a single layer of Ink B inkjet printed onto transfer tattoo paper. (a) shows the multilayer structure of the transfer tattoo paper with three distinguishable layers; (b) shows a closer look to the upper layers of transfer tattoo paper onto which a single layer of Ink B has been inkjet printed; (c) and (d) show the cross-section a silver film inkjet printed onto transfer tattoo paper heated for 15 and 90 minutes, respectively.

heating, with the exception of features comprising 2 layers of ink and printed at 15 μm dot spacing (thicker features), resistivity increases abruptly for all inkjet printed features. The increase in resistance is more pronounced for thinner features. After 60 minutes sintering the resistivity of all features increases even further. Features with 1 layer of ink printed at 20 μm dot spacing become non-conductive.

Fig. 4a and b show scanning electron microscopy (SEM) images of the cross-section of a single layer of silver ink on tattoo paper. Four layers are clearly visible: the top white layer of approximately 1 μm thickness corresponds to the silver film. Fig. 4b suggests ink penetration into the ink receiving layer was minimal. This could be due to the structure of the ink-receiving layer, which could have been designed to minimize ink wicking, and/or caused by the fast evaporation of solvent since printing is being carried out on a heated substrate, with the three layers underneath the silver film correspond to the transfer paper. Fig. 4c and d correspond to SEM images of the cross-section of tattoo paper samples onto which a single layer of silver ink was inkjet printed and subsequently sintered for 15 and 90 minutes, respectively. Fig. 4c shows a continuous silver film whereas Fig. 4d shows a discontinuous silver film with multiple cracks. We suspect the nature of these cracks could be related to deformation of the ink-receiving layer upon heating. It has been reported in the literature that photo-paper ink-receiving layers are based on polymers such as polyvinyl acetate (PVAc, T_g 30 °C), polyvinyl alcohol (PVA, T_g 85 °C), CMC (T_g 160 °C), gelatin (T_g approx. 200 °C) or microporous layers based on silica, or a combination of both are widely used.[20] We analyzed the ink-receiving layer of tattoo paper by differential scanning calorimetry (DSC), aiming at determining the glass transition temperature (T_g), and also by FT-IR. DSC results were inconclusive and a T_g couldn't be determined suggesting the ink-receiving layer of tattoo paper might be a mixture of compounds, supported by the various transition steps observed in its TGA described in Fig. 1b. FI-IR spectrum of the ink receiving layer (see FT-IR in the ESI†, Fig. 2) shows peaks which could be assigned to PVA polymer to PVA. Furthermore, the TGA of PVAc reported in the literature resembles that showed in Fig. 1b.[21] Therefore, we are inclined to think the ink-receiving layer of tattoo paper is possibly a mixture of PVA and PVAc and possibly has T_g value lower than 135 °C. We suspect the low T_g of the ink-receiving layer combined with 90 minutes heating time resulted in deformation of the ink-receiving layer and, subsequently, the formation of cracks within the thin silver film. It has been previously reported that the presence of cracks in conductive structures is a major cause of decreased conductivity.[22] Although Fig. 4c does not show the formation of cracks at the surface of the silver film it is possible that, after only 15 minutes heating, cracks were present at the bottom of the silver film which interfaces with the ink-receiving layer. This could explain the higher values of resistance obtained for features printed under the same conditions and heated up for the same amount of time on tattoo paper compared to glass, as shown in Fig. 3. Although differences in electrical performance have been reported for conductive lines printed onto different substrates with different thermal conductivity[23] and this might have been a contributing factor to differences in resistivity profiles between glass and tattoo paper printed samples, we strongly believe the deformation of the ink-receiving layer was the major contributor to the differences in electrical performance between glass and paper samples. This is supported by the substantial resistance increase for thinner tattoo paper samples heated for over

45 minutes, Regime II, as shown in Fig. 3. Unlike on glass substrates where a decrease in resistivity is observed as the length of the sintering time increases, on tattoo paper, with the exception of a line consisting of 2 layers of ink printed at 15 μm dot spacing, all lines sintered for more than 45 minutes showed an increase in resistance. It was observed the longer the sintering time the higher the resistance with thinner lines (1 layer, 20 μm dot spacing) showing the highest values of resistance. A single layer line on tattoo paper printed at 20 μm dot spacing heated for 90 minutes showed no conductivity. These results agree with previous findings reporting how thicker conductive prints remain more conductive than thinner prints upon the formation of cracks within the structure caused by the deformation of the underlying substrate.[22] Based on these findings, in order to minimize the impact the degradation of the ink-receiving layer of tattoo paper on the electrical performance of inkjet printed conductive features, inkjet printed RFID tags were sintered at 135 °C for 30 minutes only.

To demonstrate the potential applicability of inkjet printing as a powerful tool to fabricate low cost passive UHF RFID tags on tattoo paper, UHF RFID antennas of the structure depicted in Fig. 5a were inkjet printed. Nominal antenna dimensions (in mm) are: $L = 65$, $W = 20$, $l = 14.5$, $w = 3$ and $t = 0.5$. Details of fabrication by etching and stencil printing means, design considerations, simulated electrical flow within the antenna and their read range performance upon transfer onto skin have been reported somewhere else.[11] An image of an inkjet printed UHF RFID tattoo tag upon transfer onto a volunteer's arm is shown in Fig. 5b. A first iteration of inkjet printed antennas comprising 1, 2 and 3 ink layers (named 1, 2, 3 full antenna) were produced. Sintering was performed when all ink layers had been deposited. After thermal sintering, antenna port-to-port resistance (R_{p2p}) was measured. In order to fabricate the tag, a commercially available integrated circuit (IC) chip of specific impedance ($14.8 + j128$ ohm) was manually attached to the ports of the antenna. Subsequently, following the procedure described in Fig. 1a, the tag was transferred onto a volunteer's arm, as shown in Fig. 5b. Maximum read distance of the UHF RFID tag upon transfer was measured (initial read distance). Read distance was evaluated every hour whilst the volunteer engaged in routine office activities for a period of 8 hours, a standard working day. In terms of tag performance over time, the majority of the tags tested on the volunteer's arm did not change performance (read range distance) within an eight hour measurement regime. This result indicates that tags were mechanically robust enough to be used in a real life environment.

Table 1 summarizes R_{p2p} and the initial tag read distance within designated UHF RFID bands for various inkjet printed tags. For comparison, R_{p2p} and read distance of etched and stencil printed tags are also illustrated. It can be seen, R_{p2p} of inkjet printed antennas decreased as the number of silver layers increased (1, 2, 3 full antenna). R_{p2p} is dependent upon the direct current resistance of the printed antenna. As shown earlier, the more layers and the shorter the dot spacing of inkjet printed features on tattoo paper heated up to 30 minutes the lower the resistivity. According to the equation $R = \rho L/A$, decreased resistivity (ρ) and increased area (A) are expected to result in a decrease of antenna resistance (R) and, subsequently, in a decrease of R_{p2p}. The R_{p2p} of antennas etched from copper sheet was considerably lower than that obtained for inkjet printed antennas due to the low bulk resistivity of copper, $1.68 \times 10^{-8}\ \Omega$ m, and the thickness of etched antennas (17 μm) which is considerably higher than that for inkjet printed antennas (approx. 1–5 μm). Therefore, R_{p2p} for etched antennas was expected to be lower than that for inkjet printed antennas.

Both, antenna image quality and R_{p2p} have an impact on the read distance. Better image quality (good antenna edge definition) improves energy coupling between the antenna and the RFID integrated circuit chip while lower R_{p2p} of the metal antenna will reduce resistive loss to heat, and hence the tag read distance is expected to increase. Therefore the lower resistivity associated with thicker conducting layers is beneficial due to increased read efficiency and the R_{p2p} of inkjet printed antennas could potentially be decreased by increasing the number of printed layers. However, this will increase the volume of ink employed to fabricate the antenna resulting in more expensive inkjet printed tags. In addition to this, we also aim to minimize tag thickness to make it less intrusive to the end user and facilitate over printing by conventional artwork.

As illustrated in Table 1, the read distance of the first iteration of inkjet printed tags increases from 12 up to 54 cm as the number of printed layers increases from 1 up to 3 (full antennas). However, despite inkjet printed antennas with 2 layers of ink (2 full antenna) resulting in better image quality and lower R_{p2p} than stencil printed antennas, the maximum read distance obtained for an inkjet printed tag, 37 cm, was shorter than that for a stencil printing tag, 45 cm, which is maybe a consequence of two possible effects. Firstly the process to attach the IC chip onto the antenna ports causing some cracks in the antennas subsequently increasing R_{p2p} of the inkjet printing antenna and resulting in poor ohmic contact. Or secondly, According to Table 1 the silver paste tag has a high read range for its R_{p2p} (27 Ω) when compared to the 2 layer inkjet tag (14 Ω). This is because the paste and inkjet ink had significantly different conductor thicknesses. The skin depth[23] requirement is not adequately satisfied for the 1 and 2 layer inkjet printed tags which increases the losses at high frequencies compared to those associated with R_{p2p} Direct Current (DC) resistive measurements. The skin depth evaluates how deeply into a conducting material a high frequency electromagnetic

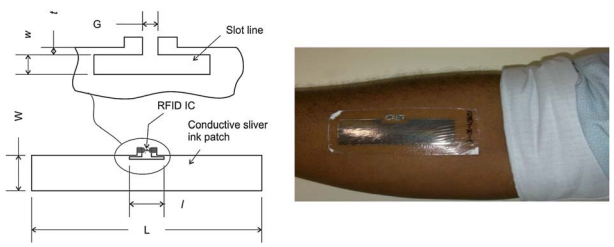

Fig. 5 UHF RFID tag schematic (left). Inkjet printed UHF RFID tag upon transfer onto the body (right).

Table 1 Different types of passive UHF RFID tags have been fabricated. The conductive material employed, fabrication method, number of silver nanoparticulate ink layers deposited to fabricate the antenna, the antenna port-to-port resistance and the initial UHF RFID tag read range upon transfer on the body are shown for comparison

Material	Fabrication method[a]	Number of ink layers	Antenna R_{p2p} [ohm]	Initial read distance[b] [cm]
Ink B	ijp	1 full antenna	116	12
Ink B	ijp	2 full antenna	14	37
Ink B	ijp	3 full antenna	11	54
Ink B	ijp	2 full antenna + 1 feed line and ports	17	59
Ink B	ijp	2 full antenna + 2 feed line and ports	4	63
Ink B	ijp	2 full antenna + 3 feed line and ports	3	68
Silver paste	Stencil	1 full antenna	27	45
Cu metal	Etching	1 full antenna	0.17	75

[a] ijp = inkjet printing. [b] Within designated UHF RFID bands: 865–868 MHz for Europe and 902–928 MHz for North America.

field will penetrate, and is inversely proportional to the square root of frequency and conductivity. Therefore, at frequencies such as those used in UHF RFID, conductors with poor R_{p2p} must be thicker than highly conducting materials if they are to avoid losses due to skin depth penetration. Assuming an inkjet ink conductivity of 33% of bulk silver, the skin depth at 900 MHz is 3.7 μm which is more than twice the height of 1 ink layer, roughly equal two 2 layers and 2/3 that of three layers. Since the thicknesses of etched copper (10 s of μm) and stencil printed pastes (100 s of μm) are considerably greater than inkjet printed tags, they are significantly less susceptible to increases in high frequency conductor loss. The conductivity of silver paste could be 10 000 times lower than bulk silver and still have high frequency performance comparable with inkjet tags due to the high paste thickness inkjet printed tags with 3 layers of ink (3 full antennas) yielded larger read distance, 54 cm, than stencil tags, 45 cm, due to the lower R_{p2p} and better resolution of the inkjet conductor deposition compared to stencil printed tags. As a benchmark, the bulk copper etched tag with a very low R_{p2p} (0.17 Ω) and high image quality, achieved a read distance of 75 cm.

In an attempt to make the ports of the inkjet printed antennas more robust and minimize a potential R_{p2p} increase upon attaching the IC chip, a second iteration of antennas was inkjet printed. This second family consisted of 2 layers of the full antenna pattern, and further ink layers deposited only in specific areas of the antenna: the feed lines and ports. We refer to this tags as 2 full antenna + x feed line and ports ($x = 1$, 2 or 3 further layers of ink). Sintering was performed when all layers had been deposited. As can be seen in Table 1, R_{p2p} decreased and read distance increased as the number of deposited layers in the feed-line and ports increased. If we compare the read range of the second iteration of inkjet printed tags with a tag consisting of only 2 layers of ink, as shown in Table 1, a substantial improvement in read distance was observed by selective depositing small amount of ink at specific areas of the tag. Furthermore, the read distance of the second iteration of tags improved compared to the best read distance value obtained from a tag comprising 3 layers of full antenna pattern. This is an important observation and results from the fact that current densities are highest in the thin conducting lines (feed lines) immediately attached to the RFID IC chip. Depositing additional printed layers in these areas of the antenna requires little extra ink, but provides a significant enhancement in UHF RFID read efficiency. This is an exceptional example of the flexibility and versatility of inkjet printing for fast prototyping and for the deposition of functional materials in specific locations in a timely fashion without the need of masks or stamps. The volume of silver ink used per tag by selective deposition of silver ink was calculated to be 32–33% less than that required to fabricate the best performing tag comprising 3 complete layers (×3 full antenna).

4 Conclusions

In summary, we have demonstrated that by choosing the appropriate ink, printing and thermal processing settings UHF RFID transfer tattoo tags functional in a real life scenario can be produced by inkjet printing means. Furthermore, by selectively depositing ink on specific areas of the tag, the read distance of inkjet printed tags was substantially larger than the read distance of stencil tags and approximating that of etched tags. In addition to this, selective ink addition resulted in a reduction of ink usage per tag, offering lower tag costs. Furthermore, inkjet printed tags are much thinner than etched or stencil printing tags thus, making them less noticeable, more comfortable and therefore more appealing to the end user. Following these initial encouraging results we believe inkjet printing of passive UHF RFID transfer tattoo tags can potentially be used to mass-produce tags at a commercially viable price. Further work is now underway to step towards commercialization. This involves modifying tag designs to improve tag performance and reduce costs, optimizing ink and substrate choice and exploring various sintering methodologies compatible with large-scale production.

Acknowledgements

Veronica Sanchez-Romaguera, Mohamed A. Ziai and Dumtoochukwu Oyeka would like to thank EPSRC for funding (EP/J000825/1). The authors also would like to acknowledge Dr Daniel J. Tate for grazing angle FT-IR measurements.

References

1 V. D. Hunt, A. Puglia and M. Puglia, *RFID: a guide to radio frequency identification*, Wiley-Blackwell, New Jersey, USA, 2007.
2 Intelleflex_RFID, Personnel Monitoring [Online]. Available: http://www.intelleflex.com/Solutions.PM.asp.
3 Motorola_RFID, "Motorola's healthcare mobility solutions," Improving Patient Safety at the Point of Care in Theatre and in Hospitals [Online]. Available: http://www.motorola.com/web/BusinessSolutions/Federal%20Government/_Documents/Static%20files/Fed_Healthcare_AB_FINAL.pdf?localeId=33.
4 H. Lehpamer, *RFID Design Principles*, Artech House Inc., Norwood, USA, 2nd edn, 2007.
5 C. Char, *Int. J. Electron. Healthc.*, 2007, **3**, 175.
6 J. G. Webster, *Medical Instrumentation: Application and Design*, Wiley, New York, USA, 2009.
7 A. Searle and L. Kirkup, *Physiol. Meas.*, 2000, **21**, 271.
8 D.- H. Kim, N. Lu, R. Ma, Y.-S. kim, S. Wang, J. Wu, S. M. Won, H. Tao, A. Islam, K. J. Yu, T.-I. Kim, R. Chowdhury, M. Ying, L. Xu, M. Li, H.-J. Chung, H. Keum, M. McCormick, P. Liu, Y.-W. Zhang, F. G. Omenetto, Y. Huang, T. Coleman and J. A. Rogers, *Science*, 2011, **333**, 838.
9 B. Davarcioglu, *International Journal of Science and Advanced Technology*, 2011, **1**, 12.
10 M. Ziai and J. Batchelor, *IET Microwaves, Antennas & Propagation*, 2010, **4**, 390.
11 M. Ziai and J. Batchelor, *IEEE Trans. Antennas Propag.*, 2011, **59**, 3565.
12 M. A. Ziai and J. C. Batchelor, *Proc. 5th European Conference on Antennas and Propagation (EUCAP)*, Rome, Italy, 2011, p. 3811.
13 G. Orecchini, F. Alimenti, V. Palazzari, A. Rida, M. M. Tentzeris and L. Roselli, *IET Microwaves, Antennas & Propagation*, 2011, **5**, 993.
14 S. Kim, M. Riccardo, M. Bozzi, S. Nikolaou and M. M. Tentzeris, *Proc. 7th European Conference on Antennas and Propagation (EUCAP)*, Sweden, 2013, p. 1870.
15 H. F. Abutarboush and A. Shamim, *Proc. 7th European Conference on Antennas and Propagation (EUCAP)*, Sweden, 2013, p. 2986.
16 Y.-W. Ju, J.-H. Park, H.-R. Jung, S.-J. Cho and W.-J. Lee, *Mater. Sci. Eng., B*, 2008, (1), 7.
17 http://www.novacentrix.com/sites/default/files/files/Metalon%20JS-B25HV%202227_2%281%29.pdf.
18 http://www.sigmaaldrich.com/catalog/product/aldrich/719048?lang=en&region=GB.
19 I. Reinhold, C. E. Hendricks, R. Eckardt, J. M. Kranenburg, J. Perelaer, R. R. Baumann and U. S. Schubert, *J. Mater. Chem.*, 2009, **19**, 3384.
20 M. Frenkle, in *The Chemistry of Inkjet Inks*, ed. S. Madgassi, World Scientific, Singapore, Thailand 2010, ch. 5.
21 J. Perelaer, C. E. Hendriks, A. W. M. de Laat and U. S. Schubert, *Nanotechnology*, 2009, **20**, 165303.
22 V. Sanchez-Romaguera, M. B. Madec and S. G. Yeates, *Materials Research Society Symposium Proceedings*, Spring Fall, San Francisco, USA, 2009, Paper: 1192-PP14-04.
23 D. M. Pozar, *Microwave Engineerin.*, John Wiley & Sons Inc., New York, 4th edn, 2012.